J|A|C|S ARTICLES

Published on Web 09/27/2010

Au Nanocube-Directed Fabrication of Au−Pd Core−Shell Nanocrystals with Tetrahexahedral, Concave Octahedral, and Octahedral Structures and Their Electrocatalytic Activity

Chun-Lun Lu, Kariate Sudhakara Prasad, Hsin-Lun Wu, Ja-an Annie Ho, and Michael H. Huang*

Department of Chemistry, National Tsing Hua University, Hsinchu 30013, Taiwan

Received June 21, 2010; E-mail: E-mail: hyhuang@mx.nthu.edu.tw

Abstract: In this study, we have successfully developed a facile method for the high-yield fabrication of Au−Pd core−shell heterostructures with an unusual tetrahexahedral (THH) morphology using Au nanocubes as the structure-directing cores. The lattice orientations of the Au nanocubes match those of the Pd shells. Structural analysis establishes that the THH nanocrystals are bounded by high-index {730} facets. A substantial lattice mismatch between Au and Pd, oxidative etching in the presence of chloride and oxygen, the use of cetyltrimethylammonium chloride (CTAC) surfactant, and the reaction temperature (30−60 °C) were identified to be key factors facilitating the formation of the THH core−shell nanocrystals. Intermediate products have also been examined to follow the growth process. By selecting cubic gold cores with sizes of 30−70 nm and varying the volume of the gold core solution used, THH Au−Pd core−shell nanocrystals with continuously adjustable sizes from 56 to 124 nm can be readily obtained. Their UV−vis spectra display progressive red-shifted bands. Interestingly, novel concave octahedral and octahedral Au−Pd core−shell nanocrystals can be prepared by lowering the reaction temperature and prolonging the reaction time. The concave octahedra show depressions on all the {111} faces. Electrocatalytic activity of the three Au−Pd core−shell structures for the oxidation of ethanol has been investigated. The THH nanocrystals with entirely high-index {730} facets were found to exhibit the best electrocatalytic activity. These size-tunable THH Au−Pd core−shell nanocrystals may be valuable for catalyzing other organic reactions.

Introduction

Fabrication of bimetallic and metal-semiconductor core−shell heterostructures using polyhedral metal cores to direct the growth of shells with excellent morphology control is an important but synthetically challenging task. The resulting materials can provide opportunities for the measurements of their novel physical and chemical properties with respect to the exposed surface planes and the incorporated metal cores. Most of the successful examples of this type of nanomaterials with both structurally well-defined cores and shells are bimetallic systems.[1−9] Yang et al. have used cubic Pt seeds to form Pd nanocubes, cuboctahedra, and octahedra by epitaxial overgrowth.[1] Tian et al. employed octahedral Au nanocrystals as cores to make Pd nanocubes.[2] One-step synthesis of Au−Pd nanocrystals with octahedral core and shell structures have been reported.[3] Recently, Xia and co-workers have prepared Pd−Au bimetallic nanocrystals using Pd nanocubes as cores.[4] Depending on L-ascorbic acid or citric acid used as the reducing agent, conformal or localized overgrowth of Au on the Pd nanocubes can result. For metal-semiconductor systems, the fabrication of Au−Cu_2O core−shell heterostructures with precise morphological control by using various Au nanocrystal cores such as octahedra and nanorods has been demonstrated.[10] For bimetallic systems involving gold and palladium, it would be interesting to use Au nanocubes as the structure-directing cores for the overgrowth of Pd shells as this combination has not been reported before. Because of a significant lattice mismatch between gold and palladium, the resulting Au−Pd core−shell nanocrystals may exhibit unusual morphologies and high-index facets. Nanocrystals with high catalytic activities may be obtained. In addition, maintenance of the shell morphology with varying core particle sizes is another aspect of this type of research that is rarely examined. The formation of different shell morphologies from the same core particles by simply varying the reaction conditions such as reaction temperature and time

(1) Habas, S. E.; Lee, H.; Radmilovic, V.; Somorjai, G. A.; Yang, P. *Nat. Mater.* **2007**, *6*, 692.
(2) Fan, F.-R.; Liu, D.-Y.; Wu, Y.-F.; Duan, S.; Xie, Z.-X.; Jiang, Z.-Y.; Tian, Z.-Q. *J. Am. Chem. Soc.* **2008**, *130*, 6949.
(3) Lee, Y. W.; Kim, M.; Kim, Z. H.; Han, S. W. *J. Am. Chem. Soc.* **2009**, *131*, 17036.
(4) Lim, B.; Kobayashi, H.; Yu, T.; Wang, J.; Kim, M. J.; Li, Z.-Y.; Rycenga, M.; Xia, Y. *J. Am. Chem. Soc.* **2010**, *132*, 2506.
(5) (a) Tsuji, M.; Matsuo, R.; Jiang, P.; Miyamae, N.; Uemaya, D.; Nishio, M.; Hikino, S.; Kumagae, H.; Kamarudin, K. S. N.; Tang, X.-L. *Cryst. Growth Des.* **2008**, *8*, 2528. (b) Tsuji, M.; Miyamae, N.; Lim, S.; Kimura, K.; Zhang, X.; Hikino, S.; Nishio, M. *Cryst. Growth Des.* **2006**, *6*, 1801.
(6) Seo, D.; Yoo, C. I.; Jung, J.; Song, H. *J. Am. Chem. Soc.* **2008**, *130*, 2940.
(7) Lim, B.; Wang, J.; Camargo, P. H. C.; Jiang, M.; Kim, M. J.; Xia, Y. *Nano Lett.* **2008**, *8*, 2535.
(8) Cho, E. C.; Camargo, P. H. C.; Xia, Y. *Adv. Mater.* **2010**, *22*, 744.
(9) Zhang, K.; Xiang, Y.; Wu, X.; Feng, L.; He, W.; Liu, J.; Zhou, W.; Xie, S. *Langmuir* **2009**, *25*, 1162.
(10) Kuo, C.-H.; Hua, T.-E.; Huang, M. H. *J. Am. Chem. Soc.* **2009**, *131*, 17871.

10.1021/ja105401p

without addition of another reagent to alter the pregrown core−shell particle shape is also desirable.[1]

In this study, we have successfully used Au nanocubes as the structure-directing cores to synthesize Au−Pd core−shell nanocrystals with an unusual tetrahexahedral (THH) structure in high yield. THH Pt and Pd nanocrystals with high-index {730} facets have been prepared electrochemically.[11,12] Their high electrooxidation activity toward the oxidation of formic acid and ethanol was demonstrated. Elongated THH Au nanocrystals and THH Au microcrystals have also been synthesized recently.[13,14] Crystal structure analysis and control experiments have revealed the importance of using the cubic Au cores for the formation of Pd shells with THH morphology. Growth mechanism for the formation of the THH nanocrystals has been extensively studied. We have also used Au nanocubes of different sizes to tune the dimensions of the THH nanocrystals with excellent preservation of their morphology. By simply varying the reaction temperature and time, concave octahedral and octahedral Pd nanocrystals enclosing Au nanocubes can be readily prepared. These are also novel Au−Pd core−shell heterostructures not reported before. It is highly interesting to examine the catalytic activity of relatively large and faceted Pd nanostructures.[15] Here we have compared the electrocatalytic activities of the three novel Au−Pd core−shell nanocrystals for the oxidation of ethanol. THH Pd nanocrystals were found to possess high electrocatalytic activity resulting from their high-index facets.

Experimental Section

Chemicals. $PdCl_2$ powder (Aldrich, 99%), hydrogen tetrachloroaurate trihydrate ($HAuCl_4 \cdot 3H_2O$, 99.9%, Aldrich), cetyltrimethylammonium chloride (CTAC, 95%, TCI), cetyltrimethylammonium bromide (CTAB, 98%, Alfa Aesar), sodium borohydride ($NaBH_4$, 98%, Aldrich), ascorbic acid (AA, 99.7%, Riedel-de-Haën), and sodium bromide (NaBr, UCW) were used without further purification. Ultrapure distilled and deionized water was used for all solution preparations.

Synthesis of Gold Nanocubes. The gold nanocubes were obtained following a seed-mediated synthesis method developed in our laboratory.[16] A volume of 10 mL of aqueous solution containing 2.5×10^{-4} M $HAuCl_4$ and 0.10 M CTAC surfactant was prepared. Concurrently, 10 mL of 0.02 M ice-cold $NaBH_4$ solution was made. To the $HAuCl_4$ solution was added 0.45 mL of the $NaBH_4$ solution with stirring. The resulting solution turned brown immediately, indicating the formation of gold seed particles. The seed solution was aged for 1 h at 30 °C to decompose excess borohydride. The seed particles have sizes of 3−5 nm.

The seed particles were used to grow into nanocubes. Two vials were labeled A and B. A growth solution was prepared in each of the two vials. First, 0.32 g of CTAC and 9.625 mL of deionized water were added to each vial. The vials were then kept in a water bath set at 30 °C. To both vials were added 250 μL of 0.01 M $HAuCl_4$ solution and 10 μL of 0.01 M NaBr. Finally, 90 μL of 0.04 M ascorbic acid was introduced. Total solution volume in each vial was 10 mL. The concentration of CTAC in the final solution was equal to 0.10 M. The solution color turned colorless after the addition of ascorbic acid, indicating the reduction of Au^{3+} to Au^{+} species. Next, 65 μL of the seed solution was added to the solution in vial A with shaking until the solution color turned light pink (∼5 s). Then, 25 μL of the solution in vial A was transferred to vial B with thorough mixing for ∼10 s. The solution in vial B was left undisturbed for 15 min for particle growth, and centrifuged at 6500 rpm for 10 min (Hermle Z323 centrifuge). The particles were then dispersed in 1.5 mL of this solution. The nanocubes synthesized had an average size of ∼40 nm. Smaller nanocubes with an average size of ∼30 nm were used for the electrooxidation study. They can be synthesized by adding 100 μL of the seed solution. The product was centrifuged at 8000 rpm for 10 min. Larger gold nanocubes with average sizes of ∼70 and 55 nm were also prepared to vary the sizes of the Au−Pd core−shell tetrahexahedral nanocrystals. For the growth of nanocubes with approximate sizes of 70 and 55 nm, 25 and 45 μL of the seed solution were used, and the products were centrifuged at 3000 and 6000 rpm for 10 min, respectively.

Synthesis of Au−Pd Core−Shell Tetrahexahedral Nanocrystals. First, a 10 mM H_2PdCl_4 solution was prepared by completely dissolving 0.089 g of deep brown $PdCl_2$ powder in 50 mL of 20 mM HCl solution placed in a 60 °C water bath. In a typical synthesis of the Au−Pd core−shell nanocrystals, 0.048 g of CTAC, 8.65 mL of deionized water, 0.30 mL of the Au nanocube solution, and 0.75 mL of 10 mM H_2PdCl_4 solution were introduced into a sample vial in the order listed. The vial was kept in a water bath set at 31 °C. Then 0.3 mL of 0.1 M ascorbic acid was added and the mixture was stirred. Total solution volume in the vial was 10 mL. The solution color quickly turned brown and then gray by keeping the vial undisturbed in the water bath for 30 min. Finally, the solution was centrifuged at 3000 rpm for 5 min. The volumes of the gold nanocube solution used to synthesize Au−Pd core−shell nanocrystals of different dimensions are listed in Table S1 in the Supporting Information.

Synthesis of Au−Pd Core−Shell Concave Octahedral and Octahedral Nanocrystals. In a typical synthesis of the concave octahedral Au−Pd core−shell nanocrystals, 0.048 g of CTAC, 8.65 mL of deionized water, 0.3 mL of the Au nanocube solution, and 0.75 mL of 10 mM H_2PdCl_4 solution were introduced into a sample vial in the order listed. The vial was shaken and kept in a water bath set at 10 °C. Next, 0.3 mL of 0.1 M ascorbic acid was added to the mixture and the vial was left undisturbed for 4 h. The solution was centrifuged three times at 3000 rpm for 5 min. To prepare the octahedral core−shell nanocrystals, the same reagent amounts as those used to make the concave octahedral nanocrystals were employed. However, the reaction mixture was kept at 10 °C for 2 h. After 2 h, the solution was centrifuged at 3000 rpm for 5 min. A volume of 7 mL of the top solution was withdrawn to remove some unreacted reagents, followed by addition of 8 mL of deionized water. The solution was subsequently kept in a 20 °C water bath for 20 min and centrifuged at 2500 rpm and then at 2000 rpm for 5 min each. An illustration highlighting the main differences in the procedures for making the three Au−Pd core−shell nanocrystals is given in Scheme S1 in the Supporting Information.

Electrochemical Characterization. Relative electrochemical activities of the three Au−Pd core−shell nanocrystal structures were studied by making cyclic voltammogram measurements for electrooxidation of ethanol. For particle surface area determination, a volume of 7 μL of the centrifuged Au−Pd nanocrystal solution was drop-coated on a single disk screen printed carbon electrode with a conductive track radius of 2.5 mm and allowed to dry in an oven set at 40 °C for overnight. The as-prepared electrode was then washed with Millipore water to remove loosely bound nanocrystals. The same drying and rinsing steps were applied to the nanocrystal-coated electrode for electrocatalytic activity scans. The modified electrode was subjected to continuous potential cycling between −0.2 and 1.2 V at 50 mV/s in 1 M H_2SO_4 solution.

(11) (a) Tian, N.; Zhou, Z.-Y.; Sun, S.-G.; Ding, Y.; Wang, Z. L. *Science* **2007**, *316*, 732. (b) Ding, Y.; Gao, Y.; Wang, Z.-L.; Tian, N.; Zhou, Z.-Y.; Sun, S.-G. *Appl. Phys. Lett.* **2007**, *91*, 121901. (c) Tian, N.; Zhou, Z.-Y.; Sun, S.-G. *J. Phys. Chem. C* **2008**, *112*, 19801.
(12) Tian, N.; Zhou, Z.-Y.; Yu, N.-F.; Wang, L.-Y.; Sun, S.-G. *J. Am. Chem. Soc.* **2010**, *132*, 7580.
(13) Ming, T.; Feng, W.; Tang, Q.; Wang, F.; Sun, L.; Wang, J.; Yan, C. *J. Am. Chem. Soc.* **2009**, *131*, 16350.
(14) Hsu, S. J.; Su, P. Y. S.; Jian, L. Y.; Chang, A. H. H.; Lin, I. J. B. *Inorg. Chem.* **2010**, *49*, 4149.
(15) Chen, Y.-H.; Hung, H.-H.; Huang, M. H. *J. Am. Chem. Soc.* **2009**, *131*, 9114.
(16) Wu, H.-L.; Kuo, C.-H.; Huang, M. H. *Langmuir* **2010**, *26*, 12307.

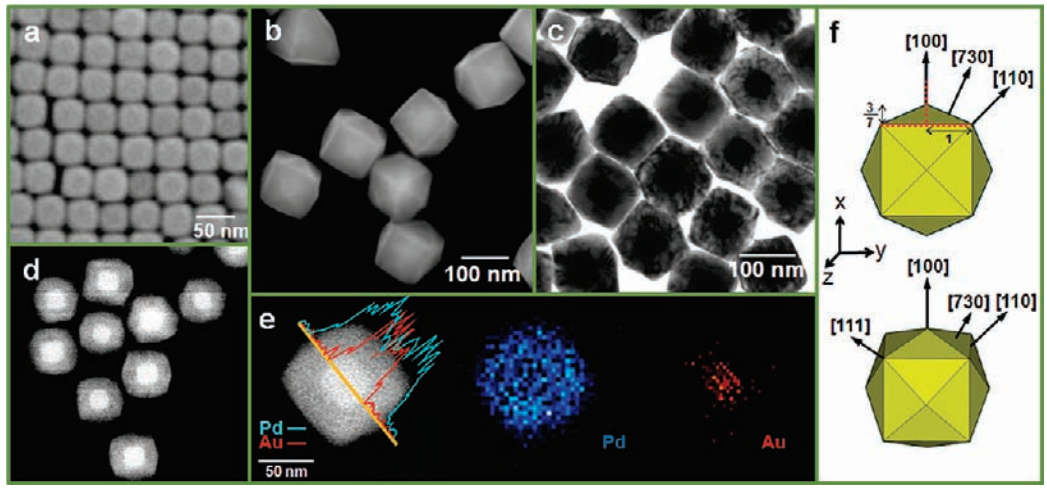

Figure 1. (a) SEM images of the cubic Au nanocrystals used to serve as the cores. (b and c) SEM and TEM images of the THH Au−Pd core−shell nanocrystals. (d) HAADF-STEM image of the THH Au−Pd core−shell nanocrystals. (e) EDS line scan and elemental mapping image of a THH Au−Pd core−shell nanocrystal. (f) Schematic drawings of a THH nanocrystal viewed from different angles. The axes projecting along the [100], [110], [111], and [730] directions are also shown. Length ratio is also shown.

For electrocatalytic activity measurements of the three nanocrystal shapes, a volume of 3 μL of the nanocrystal solution was drop-coated on an integrated three-electrode strip consisting of a carbon working electrode, a silver pseudo-reference electrode, and a carbon counter electrode, and the three-electrode strip was immersed in 0.2 M KOH solution containing 1.62 M ethanol. A scan rate of 50 mV/s was used.

Instrumentation. Scanning electron microscopy (SEM) images of the samples were obtained using a JEOL JSM-7000F electron microscope. Transmission electron microscopy (TEM) characterization was performed on a JEOL JEM-2100 electron microscope with an operating voltage of 200 kV. Elemental mapping images were acquired by energy-dispersive X-ray spectroscopy (EDS) using another JEOL JEM-2100 electron microscope equipped with a STEM unit and an Inca Energy 250 detector from Oxford Instruments. High-resolution TEM (HR-TEM) images were obtained using a JEOL JEM-3000F electron microscope. Powder X-ray diffraction (XRD) patterns were recorded on a Shimadzu XRD-6000 diffractometer with Cu Kα radiation. UV−vis absorption spectra were taken using a JASCO V-570 spectrophotometer. A Reichert-Jung Ultracut E ultramicrotome was used for making cross-section samples. Electrochemical measurements were conducted using a CH Instruments 633C electrochemical analyzer.

Results and Discussion

In this study, we consider the possibility of using Au nanocubes as the structure-directing cores for the fabrication of Au−Pd core−shell nanocrystals with well-defined product morphologies by epitaxial overgrowth of Pd. The core−shell nanocrystals can be readily prepared by mixing H_2PdCl_4 aqueous solution, CTAC surfactant, Au nanocubes, and ascorbic acid of appropriate concentrations at 31 °C for 30 min. Figure 1a shows a SEM image of the uniform Au nanocubes synthesized with an average size of ~40 nm. SEM and TEM characterization of the resulting Au−Pd core−shell nanocrystals generated using these Au nanocubes as cores for Pd shell growth are given in Figure 1. The images clearly show that the Au−Pd core−shell nanocrystals possess a tetrahexahedral structure. Average particle size was calculated to be 84 nm. The monodisperse THH Au−Pd core−shell nanocrystals have been synthesized in high yield (see the Supporting Information Figure S1). In fact, the yield of THH Au−Pd core−shell nanocrystals is nearly 100% if the cores are Au nanocubes. Byproducts such as right bipyramids of gold formed in the synthesis of gold nanocubes can slightly reduce the overall yield of THH core−shell nanocrystals.[16] Both the TEM image and high-angle annular dark-field scanning transmission electron microscopy (HAADF-STEM) image giving enhanced elemental contrast reveal a nanocube residing at the center of each THH nanocrystal. The EDS line scan and elemental mapping analyses on a single nanocrystal confirmed its Au core and Pd shell composition. Selected-area electron diffraction (SAED) pattern of a single THH nanocrystal taken over the [100] zone axis gives a square spot pattern of Pd, indicating the single-crystalline nature of the shell (see Figure S1). The facet angles determined from such TEM image suggest that the THH Au−Pd core−shell nanocrystals are bounded by the {730} surfaces (see Figure S2), a result consistent with the structural analysis carried out for the tetrahexahedral Pt nanocrystals.[11] Schematic drawings of a THH particle viewed from different directions are also provided in Figure 1.

XRD pattern of the THH nanocrystals shows relatively strong reflection peaks for Pd but weak peaks for Au, reflecting their core−shell structure (see Figure S3). Intensities of the (200) peak for both Pd and Au are slightly higher than those of the (111) peak, implying their similar orientation of deposition on a substrate to nanocubes. Cross-sectional TEM images of thin THH nanocrystal samples prepared by a microtomy technique were also taken to examine the Au−Pd interfacial region (see Figure 2). HR-TEM images show that the (200) planes of Pd grow epitaxially on the {200} faces of the Au nanocube with sharp interface, and the (220) planes of Pd also align parallel to the (220) planes of gold as seen from the nanocube corner. The (200) planes of Pd extend to the particle surface.

The formation of Au−Pd core−shell heterostructures with a THH structure bounded by 24 high-index {730} surfaces is quite unusual. Reaction conditions that promote their generation deserve interrogation. For epitaxial growth of Pd on Au nanocubes, the degree of lattice mismatch should be considered. Au and Pd have a lattice mismatch of 4.61%. This is a large mismatch compared to just 0.77% for Pt and Pd.[1] As the conformal shell growth increases in thickness, lattice strain can develop. The shell surface planes may become less regular on the atomic scale and the THH morphology with all high-index

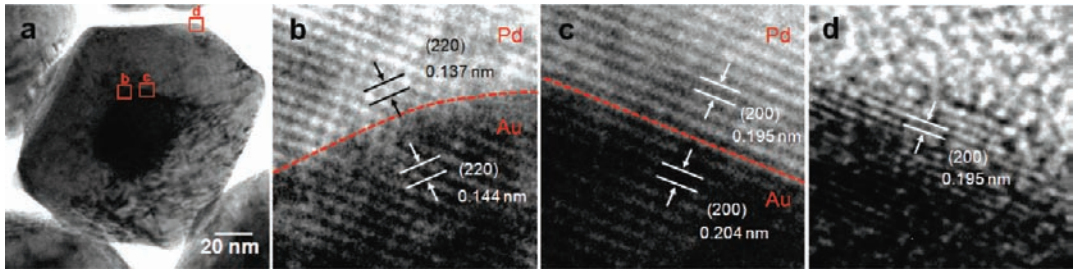

Figure 2. (a) Cross-sectional TEM image of a THH Au−Pd core−shell nanocrystal. (b−d) Interfacial HR-TEM images of the square regions shown in panel a.

facets results to respond to the build-up of this lattice strain. The necessity of using polyhedral Au nanocrystal cores of a sufficiently large size for the formation of THH nanocrystals is established in control experiments without the addition of Au nanocubes during particle growth (see Figure S4). THH nanocrystals cannot be synthesized; only decahedral, octahedral, and other polyhedral Pd nanoparticles were obtained. Use of octahedral and rhombic dodecahedral Au nanocrystal cores of similar sizes to the Au nanocubes can also yield THH Au−Pd core−shell heterostructures (see Figure S5). These gold cores have been prepared following our developed procedures.[16,17] The lattice mismatch values between Pd and Au (220) and (111) planes are 4.62 and 4.64%, respectively, so the formation of THH core−shell heterostructures seems reasonable. Reaction temperature also affects the development of the THH particle shape. THH nanocrystals can be synthesized at temperatures of 30 to below 60 °C. At 60 °C, Pd nanoparticles can also form.

The effect of capping surfactant used was also studied. In the absence of CTAC surfactant in the reaction mixture, irregularly shaped core−shell particles and smaller Pd nanoparticles were made. Replacing CTAC with CTAB surfactant yielded cubic-shaped Au−Pd core−shell nanocrystals (see Figure S6). The presence of bromide has been suggested to promote the formation of {100} and {110} facets of Pd in the polyol process.[18] The results show that CTAC is a necessary capping surfactant for the formation of the THH Au−Pd nanocrystals. The role of chloride is likely related to the oxidative etching of Pd surface for the emergence of {730} faces via the following redox reaction:

$$Pd + O_2 + 4Cl^- + 4H^+ \leftrightarrow PdCl_4^{2-} + 2H_2O \qquad (1)$$

To validate this mechanism, the reaction mixture without ascorbic acid was purged with nitrogen for 30 min, and then ascorbic acid was added to initiate the reaction with the vial capped and nitrogen flow injected above the solution. This procedure removes the dissolved oxygen and prevents reoxidation of the Pd shells. The Au−Pd core−shell nanocrystals formed exhibit a roughly cubic structure with irregular surfaces (see Figure S7). Evidence of lattice strain extending from the interior to the heterostructure surfaces seems apparent. The results support the role of oxidative etching in the presence of oxygen and chloride to induce the formation of sharp {730} facets. Oxidative etching has also been suggested in the hydrothermal synthesis of octahedral gold nanocrystals.[17]

Further insight into the growth mechanism can be gained by withdrawing a drop of the reaction solution to examine the intermediate products formed. Figure 3 gives the TEM images of the intermediate products observed at different reaction times to follow the reaction progress. Within 5 s, a very thin Pd shell has formed on the Au nanocube surface. The TEM image taken after 60 s of reaction shows that the developing core−shell nanocrystal is surrounded by many twisted Pd nanostructures. These twisted Pd nanostructures appear to concentrate toward the Au surface. Some Pd nanoparticles are also found, and they should aggregate toward the larger Au nanocrystals. Thus, the shell growth process partially follows the Ostwald ripening mechanism. Within 180 s, a thick Pd shell has already been formed around the Au core possibly from these twisted nanostructures, although the shell coverage is not uniform. Neighboring ultrasmall Pd nanoparticles surrounding the developing core−shell heterostructure were found to orient with their (111) lattice fringes aligned parallel to each other and roughly parallel to the Au (111) planes (see Figure 3cl and e1). The observation suggests that the epitaxial shell growth may involve oriented deposition of Pd particles on the Au core surface. Regardless of the exact forms of Pd source, epitaxial shell growth should have established as soon as the Pd shell is formed. Shell growth is mostly complete in 5 min, but sharp facets are not yet developed; the core−shell nanocrystals then evolve into a THH morphology via surface reconstruction after 5 more min of reaction. This rapid crystal growth followed by a period of surface reconstruction to yield well-defined structures has also been observed for Cu_2O nanocrystals.[19]

On the basis of the above mechanistic studies, a schematic illustration of the formation of {730} surface is presented in Scheme 1. The Pd shell formed via Ostwald ripening may be more strained due to a lattice mismatch of 4.61% between cell parameters of Au and Pd. In the presence of dissolved oxygen and chloride ions, continuous Pd atom reduction and partial oxidative etching may occur during Pd particle deposition. Oxygen atoms dissolved in water may be incorporated into the lattice as a result of unsaturated coordination of surface Pd atoms and subsequently removed in the redox cycle.[11a] Steps, ledges, and kinks created by the oxidative etching process are protected by surfactant as CTAC may adsorb more strongly to these sites with lower Pd coordination numbers. Consequently, high-index faces are formed.

Variation of the particle size for core−shell nanocrystals with polyhedral cores and shells while preserving the product morphology has rarely been demonstrated. Here dimensions of the THH nanocrystals can be easily tuned by using Au nanocubes with sizes of 30, 40, 55, and 75 nm and adjusting

(17) Chang, C.-C.; Wu, H.-L.; Kuo, C.-H.; Huang, M. H. *Chem. Mater.* **2008**, *20*, 7570.
(18) Xiong, Y.; Cai, H.; Wiley, B. J.; Wang, J.; Kim, M. J.; Xia, Y. *J. Am. Chem. Soc.* **2007**, *129*, 3665.
(19) Kuo, C.-H.; Huang, M. H. *J. Phys. Chem. C* **2008**, *112*, 18355.

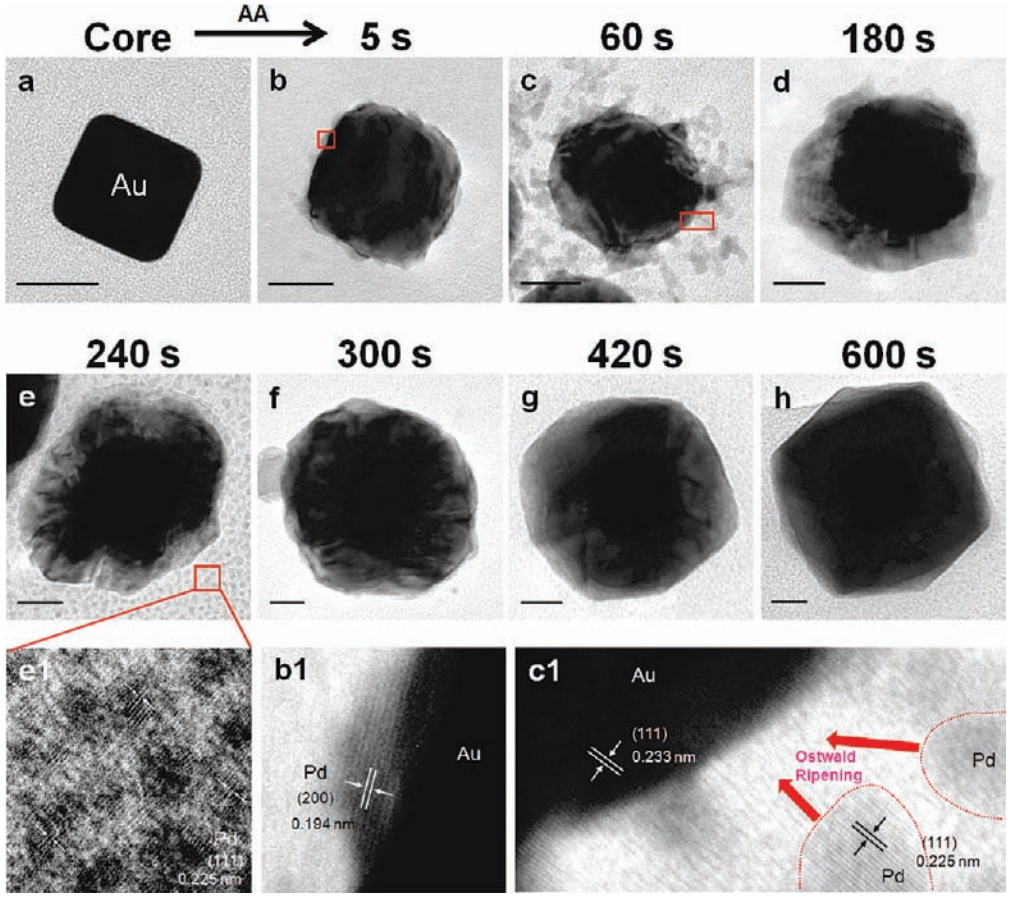

Figure 3. (a) TEM image of a Au nanocube. (b−h) TEM images of the Au−Pd core−shell heterostructures taken at different times after the addition of ascorbic acid to disclose the formation process of the THH nanocrystals. Scale bar is equal to 20 nm for every image. (b1) Enlarged TEM image of the square region in panel b showing a thin Pd shell. (c1) TEM image of the rectangular region in panel c. Pd particles appear to aggregate toward the Au nanocube surface to form the shell. A Pd particle has its (111) lattice fringes oriented nicely to the (111) lattice planes of Au. This growth process is consistent with the Ostwald ripening mechanism. (e1) Many Pd particles surround the developing Pd shell with their (111) lattice fringes aligned in the same direction.

Scheme 1. Schematic Illustration of the Formation of {730} Surface

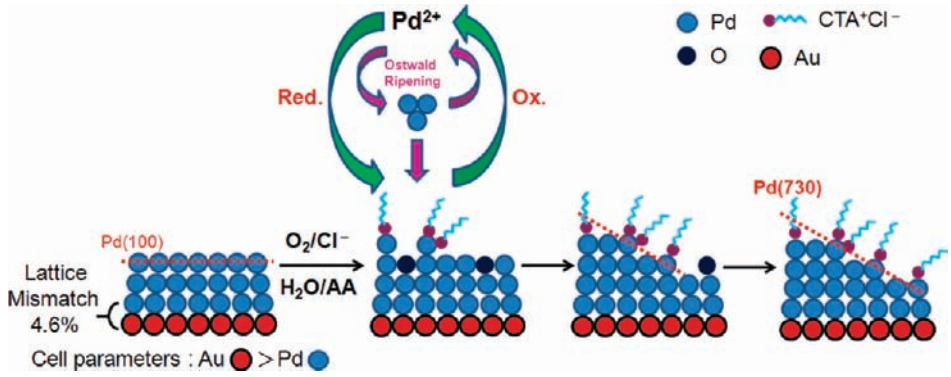

the volume of the Au nanocube solution added in the range of 250−700 μL. Figure 4 shows SEM images of the excellent THH Au−Pd core−shell nanocrystals prepared with average sizes ranging from 56 to 124 nm. All the samples displayed narrow size distributions (see Table S1 and Figure S8). To reduce the THH nanocrystal size, smaller Au cores should be selected (vice versa). Using the Au cores of a particular size, introduction of a lesser volume of the Au nanocube solution gives larger THH particles. UV−vis absorption spectra of these THH Au−Pd core−shell nanocrystals are shown in Figure 5 with the band maxima listed. Two surface plasmon resonance (SPR) absorption bands have been recorded but are not separable for the 56 and 63 nm nanocrystal samples. The spectral features are due to SPR absorption of Pd, since the Au nanocubes display only a single SPR absorption band with maxima going from 532 nm for the 30 nm cubes to 575 nm for the 70 nm cubes.[16] Progressive band red-shifts are evident as the core−shell nanocrystals increase in size. Large band red-shifts have also been observed for Pd nanocubes of different sizes from 22 to 109 nm.[20] The appearance of two absorption bands is associated with the special geometry of the Pd shell. The progressive band red-shift should also be related to the changes in the shell

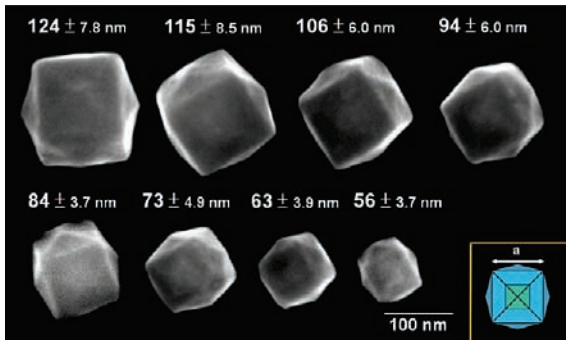

Figure 4. Representative SEM images of the THH nanocrystals synthesized with sizes varying from 56 to 124 nm. The particle size listed is equal to length a in the inset model.

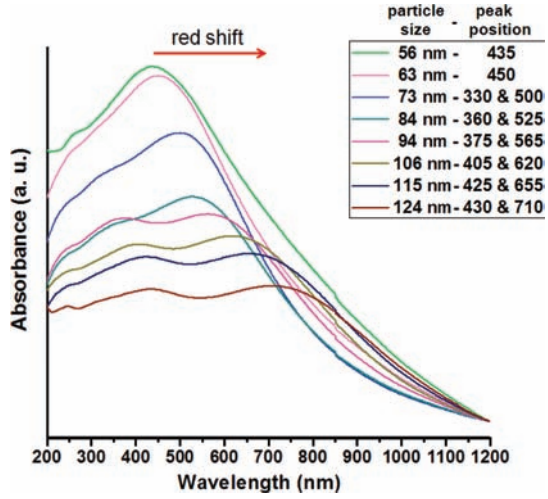

Figure 5. UV−vis absorption spectra of the THH Au−Pd core-shell nanocrystals with average lengths from 56 to 124 nm. Peak positions are also listed.

thickness and the size of the shell layer; the 73, 84, and 94 nm nanocrystal samples all used 40 nm Au nanocube cores. The tiny band at 250−265 nm is attributed to the CTAC-$PdCl_4^{2-}$ mixture.[21]

Interestingly, concave octahedral and octahedral Au−Pd core−shell nanocrystals can be prepared by using the same synthetic procedure and reagent concentrations as those employed for the growth of the THH nanocrystals but changing the reaction temperature and time (see Scheme S1). The THH nanocrystals examined in this study have been synthesized by keeping the reaction mixture at 31 °C for 30 min. Concave octahedral core−shell nanocrystals can be obtained by lowering the reaction temperature to 10 °C for 4 h. Panels a and b of Figure 6 are the SEM images of the concave octahedra formed using the 40 nm Au nanocube cores. The particles are monodisperse in size. The product yield is also nearly 100% if the cores were gold nanocubes. Every face of the octahedral nanocrystals shows a depression. Their XRD pattern gives essentially the (111) reflection peaks of Pd and Au, reflecting their dominant {111} faces parallel to the substrate surface (see Figure S3). Figure 7 presents the SEM and TEM images of individual concave octahedral nanocrystals viewed along the [100], [110], and [111] directions. The SAED patterns match those of Pd. The angle formed between a depressed side face and an octahedral face of a concave octahedral nanocrystal when viewed down the [110] direction gives an angle of 54°, suggesting the depressed side faces are the {100} faces (see Figure 7e,f). Analysis performed in Figure 7c shows that the depressed faces are parallel to the Au nanocube faces, further indicating the depressed side facets as the {100} facets. Schematic drawing of a concave octahedral Au−Pd core−shell nanocrystal with the facets labeled is available in the Supporting Information (Figure S9).

A route to fill the depressed faces by promoting growth over the {111} faces has been found. Figure 6 displays also the SEM and TEM images of the resulting octahedral Au−Pd core−shell nanocrystals prepared by using the same conditions as those employed to make the concave octahedra, but keeping the solution at 10 °C for just 2 h and then at 20 °C for 20 min with removal of the top solution and addition of water between the temperature change. The octahedral core−shell nanocrystals are uniform in size and shape that they spontaneously form a self-assembled monolayer on the substrate. The octahedra do not always possess sharp faces; faults and defects can appear as a manifestation of the lattice strain. Because of ordered packing structure, their XRD pattern also exhibits only the (111) reflection peaks of Pd and Au (see Figure S3). The SAED pattern taken along the [111] zone axis matches that of Pd as well. At 10 °C, the shell growth rate is slower, as evidenced by a much longer reaction time needed to make the core−shell nanocrystals. This relatively slow growth rate does not favor the formation of the THH nanocrystals, and typical shell morphology such as an octahedral structure with low-index facets results. The growth rate along the edges and corners of an octahedron, or along the <110> and <100> directions, may be faster than that along the faces, leading to the formation of a concave octahedron. To promote face growth and form octahedral shells, we found removal of some surfactant and palladium source in the solution to modulate the growth rate along different crystallographic directions and raising the reaction temperature to 20 °C can produce octahedral core−shell nanocrystals. Imperfect THH nanocrystals were generated using a reaction temperature of 20 °C throughout the experiment. Simply raising the temperature without the centrifugation step can yield less perfect octahedra.

The THH Au−Pd core−shell nanocrystals may exhibit a higher catalytic activity because of the presence of all high-index facets.[11,12] Electrooxidation of ethanol in KOH solution was performed to probe relative electrocatalytic activities of the three Au−Pd core−shell structures synthesized in this study. Cyclic voltammograms of the three samples in 1 M H_2SO_4 solution were obtained to determine electroactive surface areas of the electrodes (see Figure S10). Electroactive surface area of the electrode is calculated from the electric charge of hydrogen adsorption/desorption (Q_H) on Pd surfaces by adopting an assumption of 212 $\mu C/cm^2$.[12] The Q_H values for THH, concave octahedral, and octahedral nanocrystals were found to be 51.43, 72.30, and 28.65 μC, respectively (see Table S2). The electroactive surface areas of THH, concave octahedral, and octahedral nanocrystals are 0.24, 0.34, and 0.13 cm^2, respectively. The electroactive surface areas are related to the particle size and geometry. Average diameters of the THH, concave octahedral, and octahedral core−shell nanocrystals are 74, 105, and 100 nm. Figure 8 shows the cyclic voltammograms of the three Au−Pd nanocrystal-modified electrodes for ethanol oxida-

(20) Niu, W.; Li, Z.-Y.; Shi, L.; Liu, X.; Li, H.; Han, S.; Chen, J.; Xu, G. *Cryst. Growth Des.* **2008**, *8*, 4440.
(21) Berhault, G.; Bausach, M.; Bisson, L.; Becerra, L.; Thomazeau, C.; Uzio, D. *J. Phys. Chem. C* **2007**, *111*, 5915.

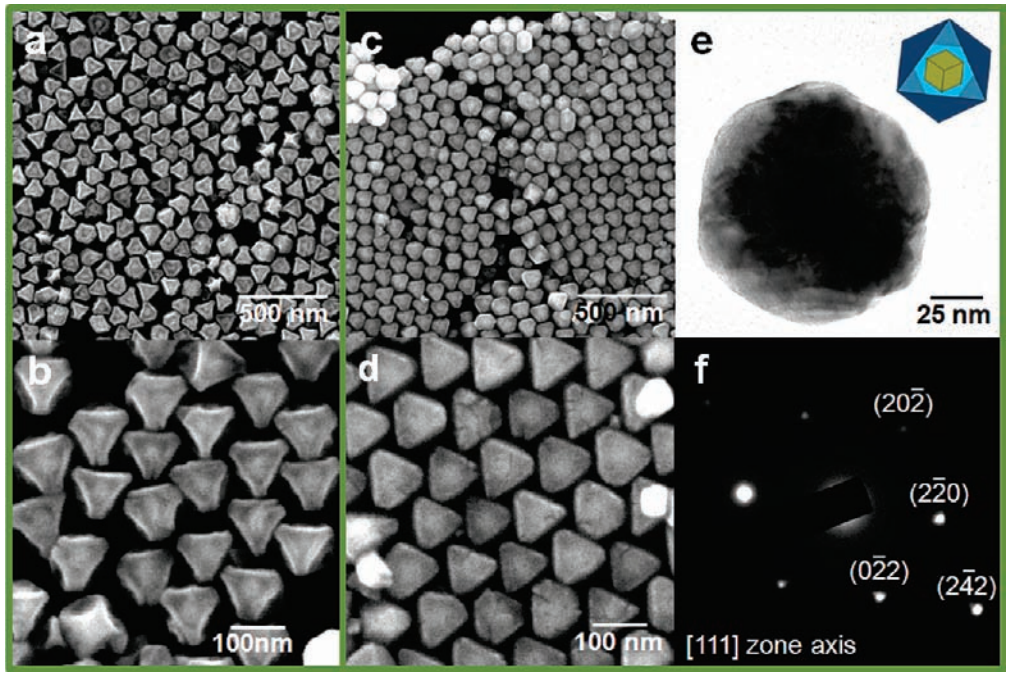

Figure 6. SEM images of (a and b) concaved octahedral and (c and d) octahedral Au−Pd core−shell nanocrystals. (e and f) TEM image of an octahedral Au−Pd core−shell nanocrystal viewed along the [111] direction and its corresponding SAED pattern. A model of the core−shell nanocrystal is also provided.

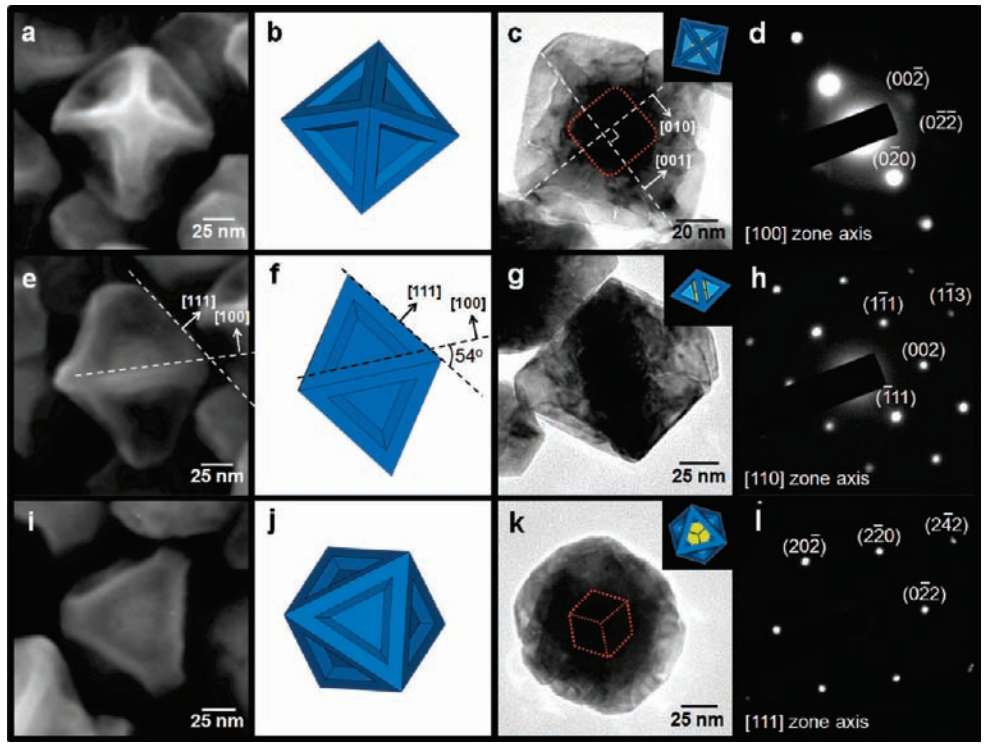

Figure 7. SEM and TEM images of the concave octahedral Au−Pd core−shell nanocrystals viewed along the [100], [110] and [111] directions. The corresponding SAED patterns to the TEM images are also shown. Schematic drawings of concave octahedral particles with their orientations consistent with the SEM and TEM images are also provided. The schematic drawings show a perfect octahedral structure for better presentation. Actually, the concaved octahedra have slightly truncated corners.

tion after electroactive surface area normalization. It is clear that the THH nanocrystals exhibit the highest electrocatalytic activity with a forward oxidation current (i_F) and a reverse oxidation current (i_R) value of 49.5 and 141.7 μA, respectively, as compared to those for the concave octahedra (i_F, 23.5 μA; i_R, 69.3 μA) and octahedra (i_F, 42.8 μA; i_R, 86.3 μA). The i_F peak current for the THH nanocrystals is around 2.1 and 1.2 times higher than those recorded for the concave octahedra and octahedra (see Table S3). The high electrocatalytic activity of the THH Au−Pd core−shell nanocrystals is attributed to the existence of all high-index {730} facets. Pd(100) surface has been shown to be the best surface for the dissociation of ethanol

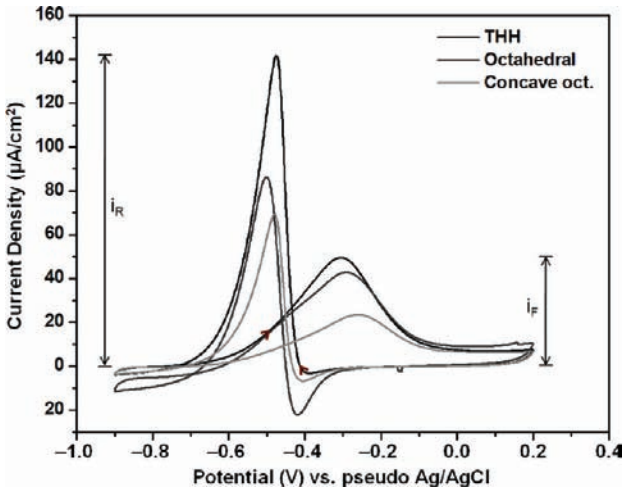

Figure 8. Cyclic voltammograms of different Au−Pd nanocrystal-modified electrodes in 0.2 M KOH solution containing 1.62 M ethanol with a scan rate of 50 mV/s for the determination of comparative electrocatalytic activities of the samples. The entire curves have been normalized to the electroactive surface areas of the three Au−Pd core−shell nanocrystal samples.

molecules among low-index planes with a low energy barrier.[22] In this regard, it is not certain why octahedral core−shell nanocrystals are more catalytically active than concave octahedra. A possibility is that the small fraction of {100} facets on the surfaces of the concave octahedra may not be so important in enhancing their electrocatalytic activity toward ethanol oxidation.

Conclusion

We have used gold nanocubes as the structure-directing cores for the fabrication of Au−Pd core−shell heterostructures possessing an unusual THH morphology with {730} facets in high yield. The core−shell structure and their composition have been verified by XRD, TEM, and EDS techniques. All the lattice planes or directions of the Au nanocube are parallel to the corresponding lattice planes or directions of the Pd shell, indicating a fixed orientation relationship between the core and the shell. A substantial lattice mismatch between Au and Pd, oxidative etching in the presence of chloride and oxygen, the use of CTAC as the capping surfactant, and the reaction temperature were found to be key factors facilitating the formation of the THH core−shell nanocrystals. TEM examination of the intermediate products reveals the formation of twisted Pd nanostructures on the Au cores and the presence of some Pd nanoparticles. By using cubic cores of different sizes and adjusting the volume of the gold core solution introduced, THH Au−Pd core−shell nanocrystals with eight progressively increasing dimensions from 56 to 124 nm were conveniently prepared. Their UV−vis spectra show progressive red-shift of the two SPR absorption bands with increasing particle size. By lowering the reaction temperature and increasing the reaction time, novel concave octahedral and octahedral Au−Pd core−shell nanocrystals can be synthesized. The concave octahedral nanocrystals were found to possess both {111} and {100} facets. Electrocatalytic activity of the THH, concave octahedral, and octahedral core−shell nanocrystals for the oxidation of ethanol has been investigated. The THH nanocrystals possessing entirely high-index {730} facets exhibit a significantly better electrocatalytic activity than that of the other two Au−Pd heterostructures with low-index facets. With the advantages of a facile synthesis method and continuously adjustable particle sizes, these THH Au−Pd core−shell nanocrystals may find applications in various Pd-catalyzed organic reactions.

Acknowledgment. We thank the National Science Council of Taiwan for the financial support of this work (NSC 98-2113-M-007-005-MY3 and NSC 98J900026).

Supporting Information Available: Schematic illustration of the synthetic conditions, additional SEM images of the THH core−shell nanocrystals, TEM images of single THH nanocrystals, XRD patterns, SEM image of Pd nanocrystals synthesized in the absence of Au nanocubes, SEM images of the THH core−shell nanocrystals synthesized using rhombic dodecahedral and octahedral gold cores, SEM images of the core−shell nanoparticles synthesized without adding CTAC or with the use of CTAB surfactant, SEM images of the products formed under nitrogen flow, table of the reaction conditions used to vary the THH nanocrystal size and the size distribution histograms, drawing of a concave octahedral nanocrystal, cyclic voltammograms for electroactive surface area determination, and tables of electroactive surface areas and peak current values for ethanol oxidation. This material is available free of charge via the Internet at http://pubs.acs.org.

JA105401P

(22) Wang, E. D.; Xu, J. B.; Zhao, T. S. *J. Phys. Chem. C* **2010**, *114*, 10489.